



Universidade de São Paulo

Biblioteca Digital da Produção Intelectual - BDPI

Departamento de Física e Ciências Materiais - IFSC/FCM

Artigos e Materiais de Revistas Científicas - IFSC/FCM

2013-11

Electrophoretic deposition of BaTi_{0.85}Zr_{0.15}O₃ nanopowders

Materials Research, São Carlos : Universidade Federal de São Carlos - Departamento de Engenharia de Materiais, v. 16, n. 6, p. 1344-1349, Nov./Dec. 2013
<http://www.producao.usp.br/handle/BDPI/45276>

Downloaded from: Biblioteca Digital da Produção Intelectual - BDPI, Universidade de São Paulo

Electrophoretic Deposition of $\text{BaTi}_{0.85}\text{Zr}_{0.15}\text{O}_3$ Nanopowders

Eduardo Antonelli^a, Ronaldo Santos da Silva^b,

Maria Inês Basso Bernardi^c, Antonio Carlos Hernandes^{c,*}

^aInstituto de Ciência e Tecnologia, Universidade Federal de São Paulo – UNIFESP,
São José dos Campos, SP, Brazil

^bGrupo de Materiais Cerâmicos Avançados, Departamento de Física, Universidade Federal de Sergipe – UFS,
São Cristóvão, SE, Brazil

^cGrupo Crescimento de Cristais e Materiais Cerâmicos, Instituto de Física de São Carlos,
Universidade de São Paulo – USP, São Carlos, SP, Brazil

Received: March 12, 2013; Revised: June 6, 2013

The present study reports the results of thick films (20-130 μm) produced through electrophoretic deposition of $\text{BaTi}_{0.85}\text{Zr}_{0.15}\text{O}_3$ (BTZ) nanometric powders synthesized by the Pechini's method. The BTZ powder calcined at 600°C/2h presented a single crystalline phase with an average particle size of ~20nm. To thick films deposition, a stable suspension of acetylacetone (Acac) and ethanol (EtOH) was prepared and the powder was deposited on platinum substrates. The viscosity of BTZ powder suspensions as a function of operational pH (OpH) was measured and the reactions between nanoparticles and the media were discussed. A milling process was used to deagglomerate the powders and it had a great influence in the suspension stability and deposition of thick films. Dense and crack-free thick films were obtained after sintering at 1220 °C/1h. The dielectric properties results, comparable with those of bulk BTZ ceramics, suggested potential applications of the EPD process for the deposition of ferroelectric/piezoelectric thick films.

Keywords: barium zirconium titanate, thick films, electrophoretic deposition, ferroelectric

1. Introduction

The study of ABO_3 -type solid solutions based on perovskite-structured barium titanate (BaTiO_3) has so far been of great interest as it offers the possibility to optimize several electrical properties for the manufacture of a number of devices, including multilayer capacitors¹. In particular, $\text{BaTi}_{1-x}\text{Zr}_x\text{O}_3$ materials have been explored, showing that, in appropriate amounts, Zr^{4+} induces an increase of the dielectric constant, tunability under biasing field and a reduction of the low-frequency dielectric losses. At a Zr content less than 8 at%, BTZ ceramics show a normal ferroelectric behavior and dielectric anomalies corresponding from cubic to tetragonal (Tc), tetragonal to orthorhombic (T2) and orthorhombic to rhombohedral (T3) phases transitions, have been unequivocally identified. As the Zr content increases, the phase transition temperatures approach each other, until, at a Zr content of ~0.15, only one phase transition exists²⁻⁴.

The achievement of BTZ nanometric particles has been studied using polymeric precursor methods⁵. Compared to the traditional solid state reaction method, the main advantage of this method is the better control of the stoichiometry, high purity, easy dopant incorporation, and formation of nanometric particles with controlled particle size^{6,7}.

Research on ferroelectric and piezoelectric thick films (thickness above 10 μm) is fundamental for the development of micro-electromechanical systems (MEMS) due to its

higher sensitivity, larger mechanical force and broader working frequency range compared to thin films⁸. The electrophoretic deposition (EPD) is an effective technique that allows the shaping of free standing objects, and also to deposit thick films on substrates starting from liquid suspensions of ceramic powders and by application of direct current (DC) potentials. This method employs the phenomenon of the movement of colloidal particles suspended in a medium when subjected to an electric field^{9,10}. Recent investigations have been undertaken on the electrophoretic deposition of barium titanate films¹¹⁻¹⁴, however, only few of these were successful in obtaining dense ceramic films with a uniform microstructure and morphology. Besides, a few works present quantitative data about the green density of the thick films^{11,12}. It is well known that the deposit thickness and the green-density are important factors to suppress stress effects during the shrinkage in the drying and sintering processes. Organic solvents such as acetylacetone (Acac) have often been used to suppress these effects due to their low surface tension¹⁵.

The Acac has been used by several authors for stabilization of suspensions^{13,16}. Nagai et al.¹⁴ had demonstrated the effectiveness of the mixed solution of ethanol and acetylacetone (20-80%) for the deposition of BaTiO_3 . These authors had attributed the increment on the mass deposition to the increasing of the electrical charges at the barium titanate particles surfaces.

*e-mail: antonelli@unifesp.br

Therefore, the objective of the present paper was to investigate the main parameters to BTZ nanoparticles deposition through the electrophoretic deposition (EPD) technique in order to obtaining thick films. To the best of our knowledge, the production of BTZ thick films by EPD is being reported here for the first time.

2. Experimental

BTZ nanometric powders were prepared through a modified polymeric precursor method, starting from zirconium citrate, titanium citrate and barium acetate solutions. Details about the powder synthesis and structural characterization can be found in Bernardi et al.⁵

To electrophoretic deposition, two different suspensions were studied: (1) BTZ+ethanol (EtOH) and (2) BTZ in a mixture of acetylacetone (Acac) and ethanol (EtOH) (1:1 volumetric ratio) (Acac+EtOH). Zirconia balls with diameter of 1.0mm and the own EtOH or Acac+EtOH solutions were used in the milling process.

The suspensions were characterized with a pH meter and a double-junction reference electrode (Analion V-640) for ethanolic solutions. However, there are no ethanolic based buffers available. Therefore, the electrode set-up was calibrated using aqueous based buffers, occasioning in an operational pH scale (OpH). The OpH values were adjusted by using HNO₃/CH₃COOH and NH₄OH for acid and alkaline ranges, respectively. Viscosity of the suspension was measured using a viscometer (Brookfield DV-III).

The depositions were made at room temperature using two platinum substrates (10 × 10 × 0.5 mm-99.5% purity, Heraeus Vectra), which were acted as a substrate (cathode) for BTZ deposition and counter electrode (anode). The substrates were encapsulated with a polymer resin (Vipi Flash Type 2, Class 1) and polished using diamond paste 1 μm and 1/4 μm. The resin was then removed and the substrates were washed with detergent, acetone, and subjected to cleaning by electrolysis (10V) using a solution of water and NaOH (100 mL/0.1 g). The electrodes were placed parallel with a separation of 15mm and voltages up to 200V (Tectrol – TCH 1500-100) were applied. Both voltage and current were monitored during the deposition process in the electrophoretic cell circuit and no appreciable variations during deposition were observed. The deposited mass on the substrates was obtained as a function of the applied voltage by weighing the platinum plates before and after the deposition (after drying of the solvent for 2 hours).

Thermogravimetric measurements (TG) of the deposited powder (treated at 90 °C/12h) were made in a temperature range of 25 °C to 800 °C, at a heating rate of 10 °C/min in synthetic air (O₂/N₂-1/4) (DTA, STA 409 Netzsch Model). The particle size of the calcined powder was examined by scanning electron microscopy (FEG – SEM, Zeiss DSM-940A equipped with a field emission gun). The morphology of the sintered thick film was examined by scanning electron microscopy (SEM) (Zeiss DSM 960). The structural investigation and phase formation were done by X-ray diffraction technique in a XRD-Rigaku Rotaflex RU-200B, using Cu_{Kα} radiation. The measurements were carried out at room temperature in continuous mode, in the 2θ range between 20° and 60°, and in steps of 0.02°.

Electrical measurements were carried out with a Solartron SI 1260 impedance/gain-phase analyzer at 1 kHz in the temperature range of 25 to 200 °C. The top gold electrodes were prepared by sputtering (3mm in diameter) and as bottom electrode was used the platinum substrate.

3. Results and Discussions

An important parameter to colloid stability determination is the Zeta Potential which is a measurement of the dispersion stability via the interactions strength of the colloid particles. This parameter provides information on the agglomeration of the particles in the suspension. The Zeta potential can also be related to viscosity of the suspension¹⁷. For instance, a high viscosity can be related to the poor disperse suspension and a low Zeta potential. Meanwhile, a low viscosity can be related with a better disperse suspension and a high Zeta potential. Figure 1a, b presents the viscosity as a function of the OpH in both EtOH and EtOH+Acac with nanoparticles (0.5 g BTZ – 100 mL liquid), respectively. Initially, the pure EtOH and the binary solution (EtOH+Acac-1:1 in volumetric ratio) were characterized with the pH meter and a double-junction reference electrode for ethanolic solutions without nanoparticles. The observed OpH were 7.3 and 6.5 in pure EtOH and binary solutions, respectively. When the nanoparticles were added in the pure EtOH (Figure 1a) the OpH shifted from 7.3 to 9.0 indicating a high interaction between the nanoparticles surface and the EtOH. Furthermore, this result also suggests that the nanoparticles have a basic character in relation to the

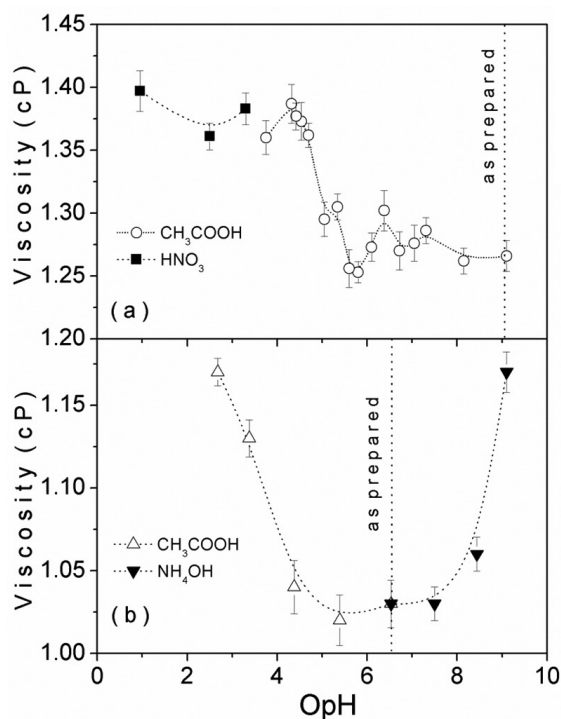


Figure 1. Effect of OpH (operational pH) on the viscosity for the (a) EtOH and (b) EtOH+Acac suspensions (0.5 g BTZ-100 mL liquid).

suspension, i.e., positive charges are absorbed. Yet, in EtOH suspensions the OpH was adjusted from 9 to 3.5 with acetic acid (CH_3COOH) and from 3.5 to 1 with nitric acid (HNO_3) additions. It was observed an increase of the suspension viscosity achieving a maximum in OpH 4 and remaining stable thereafter.

When EtOH+Acac were used (Figure 1b) the viscosity was substantially lower than that observed in Figure 1a. As suggested elsewhere^{13,16}, we can conclude that the binary solution promote a better stabilization in BaTiO_3 based materials. Considering that the nanoparticles surfaces have a basic character in relation to the solution, as soon observed, we hoped that the nanoparticles acquire positive charges and the suspension OpH became basic. Therefore, the nanoparticles will be deposited in the negative electrode, as experimentally observed. However, the OpH of the solution remains approximately constant after the nanoparticles addition (OpH 6.5). This characteristic can be attributed to the Acac addition, that in slightly basic medium can form protons $\text{CH}_3\text{CH}_2\text{OHH}(+)$ ¹⁸.

The suspension viscosity was shifted to higher values when acid acetic or ammonium hydroxide (NH_4OH) was added (Figure 1b). In fact, we have two maximums in the viscosity curve and from the electrostatic viewpoint, this result would be interpreted as two isoelectric points which is not a typical behavior for electrostatically stabilized suspensions¹⁷. Another important fact to point out is that the OpH immediately return to as prepared value (OpH 6.5) when NH_4OH is added (basic alterations).

When the powder size is reduced the surface area increases and more ions will be absorbed onto the surfaces. Besides, it is known that the increase in the H^+ ionic concentration among the particles could result in the compression of the double layer surrounding the particles. Therefore, it could lead to the lowering zeta potential, hence the colloidal stability is affected. In conclusion, the two isoelectric points observed in Figure b can be attributed to the increase in the H^+ ionic concentration among the particles, i.e., when NH_4OH (Acac in more basic medium can be form more protons $\text{CH}_3\text{CH}_2\text{OHH}(+)$ or CH_3COOH are added in the suspension, more H^+ is formed in the system. In other words, in both the cases, the H^+ ionic concentration is increased and the double layer surrounding the particles is affected.

Figure 2a shows the specific deposited weight (deposition yield) after 2 minutes as a function of the electric field applied between the platinum substrates for EtOH and Acac+EtOH suspensions (concentration of 0.5 g BTZ-100 mL liquid). As can be seen, the Acac+EtOH suspension yielded a higher mass deposition when compared to the EtOH suspension. It was also observed that the deposited powder yield changes with the applied electrical field in both suspensions, which is in accordance with the Hamaker's equation¹⁹.

The specific deposited weight (mg/cm^2) of BTZ nanoparticles on platinum substrate varying with deposition time from two concentrations of EPD suspension (5 and $10 \text{ mg}/\text{cm}^3$ (Acac+EtOH)) is shown in Figure 2b. The relation between mass deposited and deposition time is rather linear at each concentration, following also the same trend as predicted by the Hamaker's equation¹⁹. Although

the higher concentration ($10 \text{ mg}/\text{cm}^2$) to result in a higher mass deposited, the surface morphology of deposited film may become less smooth than those made from $5 \text{ mg}/\text{cm}^3$.

Figure 3 shows the specific deposited weight as a function of the ball milling time (deagglomeration) for two different applied electric fields. The thick films were deposited with EtOH+Acac suspension, nanoparticles concentration of $5 \text{ mg}/\text{cm}^3$ and deposition time of 120s. The EPD efficiency was substantially improved after ball milling for 90 min, which besides to reduce the agglomeration state also helps to introduce more proton ions from the organic solvent attached onto the ceramic powder¹³. Nevertheless, when longer ball milling time was used, we did not observe an increasing in the deposition rate, unlike, it was observed

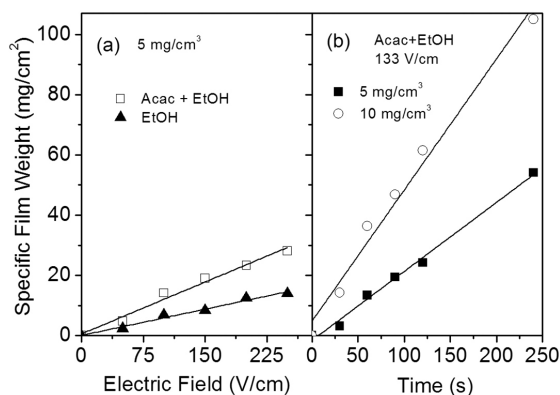


Figure 2. Specific deposited weight (deposition yield - mg/cm^2) of BTZ nanoparticles on platinum substrate varying with: (a) As a function of the electric field applied between the platinum substrates for EtOH and Acac+EtOH suspension (deposition time of 120s and concentration of $5 \text{ mg}/\text{cm}^3$). (b) Deposition time from two concentrations of EPD suspension (5 - $10 \text{ mg}/\text{cm}^3$) using the EtOH+Acac, electric field of $133 \text{ V}/\text{cm}$ and ball milling time of 120s.

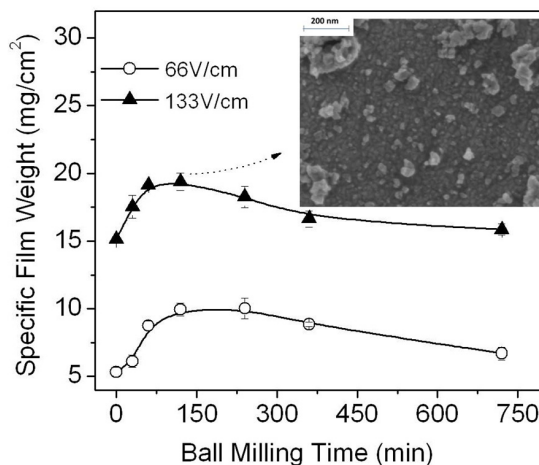


Figure 3. Specific deposited weight as a function of the ball milling time (deagglomeration) for two different electric fields applied (thick films deposited with EtOH+Acac suspension, nanoparticles concentration of $5 \text{ mg}/\text{cm}^3$ and deposition time of 120s). The insert presents a SEM micrograph of the BTZ powders deagglomerated for 2 hours.

a decrease in the mass deposited. It is commonly believed that the suspensions have its stability affected by the time (aging), for instance, Vander der Biest and Vandeperre²⁰ has suggested that for a longer ball milling the pH of the solution is shifted to point zero charge (pzc) which can be due to hydrolyze reactions and reactions between the binary solvent and solvent and nanoparticles^{10,21}. The inserted in Figure 3 presents a SEM image of the BTZ powders calcined at 600 °C/2h and deagglomerated for 2 hours in the binary solvent. The powders presented an average particle size of ~20 nm.

Figure 4 shows the XRD patterns corresponding to the BTZ15 powders (after calcination at 600 °C for 2h) and the thick film surface (after sintered at 1200 °C/1h). In both samples, calcined powder and sintered film, it was observed the formation of a single-phase compound that was identified to be isostructural with the cubic $\text{BaTi}_{0.75}\text{Zr}_{0.25}\text{O}_3$ (BTZ25) phase. The second phase observed in Figure 1b is due to the platinum substrate.

Once the film is deposited from an organic solution, it is important a slow and complete elimination of the organic material to avoid the cracks formation. Figure 5 presents the thermogravimetry (TG) curve of the deposited powder. The thick films were deposited with EtOH+Acac suspension, with nanoparticles concentration of 5 mg/cm³, for 120s and under an electric field of 133 V/cm. To TG measurements, the powder was removed from the substrate after heating at 90 °C/12h. It was observed a completely organic elimination at about 550 °C. Furthermore, as observed by Dorey and Whatmore²², one issue associated with the production of any coating on a rigid substrate is that of constrained shrinkage. The constrained shrinkage occurs when the coating undergoes a reduction in volume while the dimensions of substrate remain unchanged. This occurs during the film drying and sintering. Therefore, the principles dictating constrained shrinkage during drying and sintering are comparable. Figure 4 also shows SEM images of the green BTZ film surface deposited from the binary

suspension (EtOH+Acac) and heat treated at 90 °C/12h and 600 °C/2h, following a heating rate of 1 °C/min. It can be seen that the green form was densely packed and a porous structure was observed in both the cases.

The films thicknesses were studied by optical microscopy before and after the sintering. Figure 6

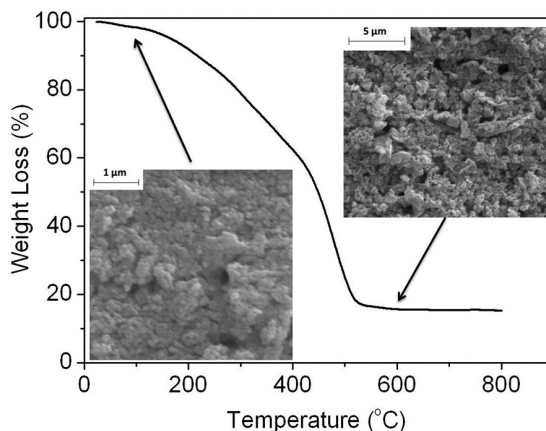


Figure 5. Thermogravimetry (TG) obtained of the deposited powder (heat treated at 90°C/12h and then removed of the substrate). The insert presents the SEM images of the surface morphology of BTZ in green form, heat treated at 90 °C/12h and 600 °C/2h. The thick films were deposited with EtOH+Acac suspension, nanoparticles concentration of 5mg/cm³, deposition time of 120s and electric field of 133V/cm.

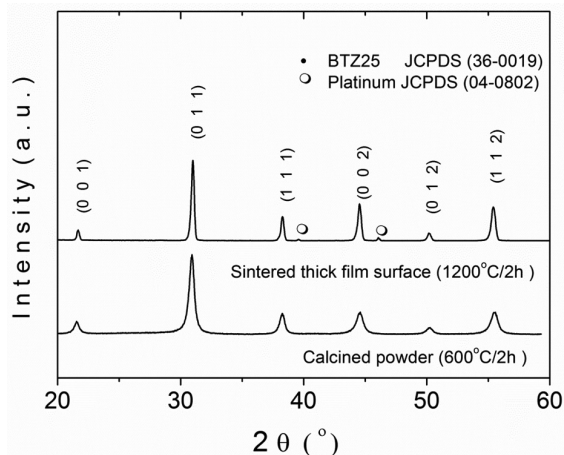


Figure 4. XRD patterns corresponding to (a) the BTZ powders (after calcination at 600°C for 2h) and (b) the thick film surface (after sintered at 1200 °C/1h) (JCPDS 36-360019 $\text{BaTi}_{0.75}\text{Zr}_{0.25}\text{O}_3$ BTZ25). The thick films was deposited with EtOH+Acac suspension, nanoparticles concentration of 5 mg/cm³, deposition time of 120s, electric field of 133 V/cm and sintered at 1220 °C/1h.

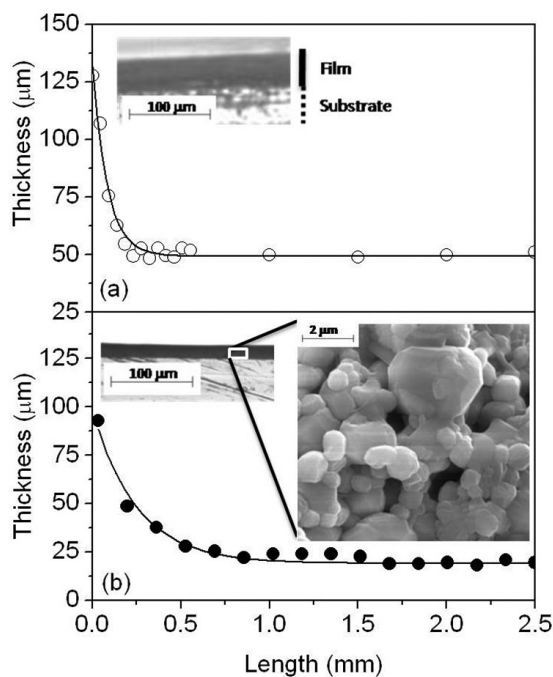


Figure 6. Thickness of the cut-cross section of the (a) deposited film and (b) sintered film at 1220 °C/1h (in detail is shown a cut-cross section and a SEM image of the thick film). The thick films were deposited with EtOH+Acac suspension, nanoparticles concentration of 5 mg/cm³, deposition time of 120s and electric field of 133V/cm.

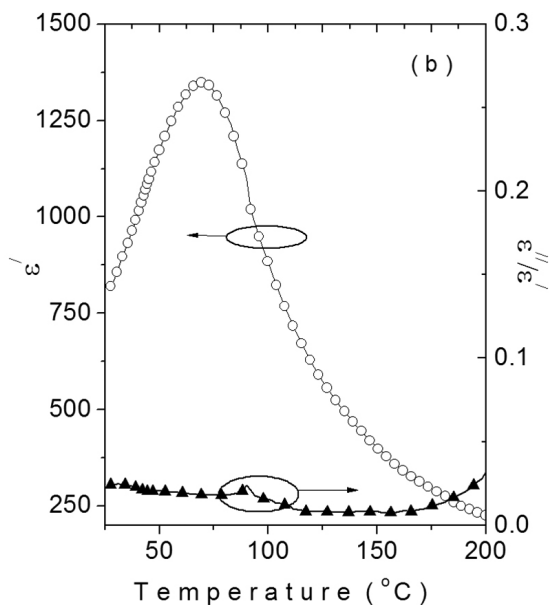


Figure 7. Temperature dependence of the dielectric constant and dielectric loss (ϵ''/ϵ') at 1 kHz. The thick films were deposited with EtOH+Acac suspension, nanoparticles concentration of 5 mg/cm², deposition time of 120s, electric field of 133V/cm and sintered at 1220 °C/1h.

presents the thicknesses of the cut-cross sections of the: (a) deposited thick film (treated at 600 °C/2h) and (b) sintered thick film at 1220 °C/1h. We can observe a constant thickness in all extension of the thick film and an edge effect (thicker deposition) in the first 200 μm . This edge effect is attributed to the electric field concentration around the edge of the exposed metal during EPD process which causes a higher powder deposition in this region²³. In detail are shown images of the thick films cut-cross section which present a homogeneous interface between the film and substrate. As can be seen (Figure 6b) the samples presented a low pores concentration and crack-free microstructure with an average grain size of (630 \pm 350) nm.

The green thick film deposited for 2 minutes and using an electrical field of 133V/cm presented thickness of

$\sim(50 \pm 5)\mu\text{m}$. As could be observed in Figure 2 the mass deposited was approximately 15mg/cm² (disregarding edge effects). Consequently, the green relative density was estimated as $\sim 50\%$ of the BaTiO₃ density ($\rho_0 = 6.02\text{g/cm}^3$). After sintered, the thickness was of (26 \pm 5) μm and the relative density was estimated in $\sim 98\%$.

Figure 7 shows the temperature dependence of permittivity and dielectric loss (ϵ''/ϵ') measured at 1 kHz for BTZ sintered thick film. The samples presented low dielectric loss values, about 3% and a single peak at 68 °C in the dielectric permittivity curve which correspond to the expected ferro-paraelectric phase transition for this BTZ composition ($x=0.15$)²⁴. In this sample, the peak value of the dielectric constant is smaller than those in bulk ceramics²⁴. It is known that the permittivity curves can be influenced by the synthesis conditions, average grain size and microstructure of the samples. However, we believed that this behavior is due to the strain of the thick film adhering to a substrate. A detailed study in this way will be done in further works.

4. Conclusions

In conclusion, barium zirconium titanate nanopowders were successfully deposited by electrophoretic technique. It was observed that Acac+EtOH solvent and an appropriate milling process presented the better condition to obtain dense, crack free and homogeneous thick films. The colloidal stability of submicron BTZ powders in solution was studied and presents an anomalous behavior when compared with micrometric powders. Dense and crack-free thick films with uniform microstructure were obtained after sintering at 1250 °C/2h. At 1 kHz, the thick films presented low dielectric loss value (3%) and ferro-paraelectric phase transition at 68 °C. Finally, these results suggested a potential application of the EPD process for the deposition of ferroelectric/piezoelectric thick films.

Acknowledgments

The authors gratefully acknowledge the financial support received by the Brazilian research funding institution FAPESP, FAPITEC, CNPQ and CAPES.

References

- Moulson J and Herbert J. M. *Electroceramics: Materials, Properties and Applications*. London: Chapman-Hall; 1990.
- Dobal PS, Dixit A, Katiyar RS, Yu Z, Guo R and Bhalla AS. Micro-Raman scattering and dielectric investigations of phase transition behavior in the BaTiO₃-BaZrO₃ system. *Journal of Applied Physics*. 2001; 89(12):8085-8091. <http://dx.doi.org/10.1063/1.1369399>
- Moura F, Simões AZ, Stojanovic BD, Zaghete MA, Longoa E and Varela JA. Dielectric and ferroelectric characteristics of barium zirconate titanate ceramics prepared from mixed oxide method. *Journal of Alloys and Compounds*. 2008; 462:129-134. <http://dx.doi.org/10.1016/j.jallcom.2007.07.077>
- Antonelli E, Silva RS and Hernandez AC. Ba(Ti_{1-x}Zr_x)O₃ ($x=0.05$ and 0.08) ceramics obtained from nanometric powders: Ferroelectric and dielectric properties. *Ferroelectrics*. 2006; 334:75-82. <http://dx.doi.org/10.1080/00150190600692591>
- Bernardi MIB, Antonelli E, Lourenço AB, Feitosa CAC, Maia LJQ and Hernandez AC. BaTi_{1-x}Zr_xO₃ nanopowders prepared by the modified Pechini method. *Journal of Thermal Analysis and Calorimetry*. 2007; 87(3):725-730. <http://dx.doi.org/10.1007/s10973-006-7767-z>
- Silva RS, Antonelli E and Hernandez AC. Low temperature synthesis and sintering of Ba_{1-x}Ca_xTiO₃ nanometric powders. *Cerâmica*. 2006; 52:168-173.
- Silva RS, Bernardi MIB and Hernandez AC. Synthesis of non-agglomerated Ba_{0.77}Ca_{0.23}TiO₃ nanopowders by a modified polymeric precursor. *Journal of Sol-Gel Science and Technology*. 2007; 42(51):173-179. <http://dx.doi.org/10.1007/s10971-007-1554-6>

8. Xu B, White D, Zesch J, Rodkin A, Buhler S, Fitch J et al. Characteristics of lead zirconate titanate ferroelectric thick films from a screen-printing laser transfer method. *Applied Physics Letters*. 2005; 87:192902. <http://dx.doi.org/10.1063/1.2126133>
9. Van der Biest O, PutS, Anné G and Vleugels J. Electrophoretic deposition for coatings and free standing objects. *Journal of Materials Science*. 2004; 39(3):779-785. <http://dx.doi.org/10.1023/B:JMSC.0000012905.62256.39>
10. Fukada Y, Nagarajan N, Mekky W, Bao Y, Kim H-S and Nicholson PS. Electrophoretic deposition - mechanisms, myths and materials. *Journal of Materials Science*. 2004; 39(3):787-801. <http://dx.doi.org/10.1023/B:JMSC.0000012906.70457.df>
11. Wu YJ, Li J, Tanaka H and Kuwabara M. Preparation of nano-structured BaTiO₃ thin film by electrophoretic deposition and its characterization. *Journal of the European Ceramic Society*. 2005; 25(12):2041-2044. <http://dx.doi.org/10.1016/j.jeurceramsoc.2005.03.008>
12. Hosokura T, Sakabe Y and Kuwabara M. Preparation of barium titanate with patterned microstructure by a novel electrophoretic deposition method. *Journal of Sol-Gel Science and Technology*. 2005; 33(2):221-228. <http://dx.doi.org/10.1007/s10971-005-5617-2>
13. Louh R-F and Hsu Y-H. Fabrication of barium titanate ferroelectric layers by electrophoretic deposition technique. *Materials Chemistry and Physics*. 2003; 79(2-3):226-229. [http://dx.doi.org/10.1016/S0254-0584\(02\)00264-X](http://dx.doi.org/10.1016/S0254-0584(02)00264-X)
14. Nagai M, Yamashita K, Umegaki T and Takuma Y. Electrophoretic deposition of ferroelectric barium titanate thick films and their dielectric properties. *Journal of the American Ceramic Society*. 1993; 76(1):253-255. <http://dx.doi.org/10.1111/j.1151-2916.1993.tb03720.x>
15. Pang X, Zhitomirsky I and NiewczasM. Cathodic electrolytic deposition of zirconia films. *Surface and Coatings Technology*. 2005; 195(2-3):138-146. <http://dx.doi.org/10.1016/j.surfcoat.2004.08.216>
16. Antonelli E, Silva RS, De Vicente FS, Zanatta AR and Hernandez AC. Electrophoretic deposition of Ba_{0.77}Ca_{0.23}TiO₃ nanopowders. *Journal of Materials Processing Technology*. 2008; 203(1-3):526-531. <http://dx.doi.org/10.1016/j.jmatprotec.2007.10.061>
17. Ma J, Zhang R, Liang CH and Weng L. Colloidal characterization and electrophoretic deposition of PZT. *Materials Letters*. 2003; 57(30):4648-4654. [http://dx.doi.org/10.1016/S0167-577X\(03\)00378-1](http://dx.doi.org/10.1016/S0167-577X(03)00378-1)
18. Wang ZH, Shemilt J and Xiao P. Fabrication of ceramic composite coatings using electrophoretic deposition, reaction bonding and low temperature sintering. *Journal of the European Ceramic Society*. 2002; 22(2):183-189. [http://dx.doi.org/10.1016/S0955-2219\(01\)00254-0](http://dx.doi.org/10.1016/S0955-2219(01)00254-0)
19. Hamaker HC. Formation of deposition by electrophoresis. *Transactions of the Faraday Society*. 1940; 35:279-287. <http://dx.doi.org/10.1039/TF9403500279>
20. Van der Biest OO and Vanderperre LJ. Electrophoretic deposition of materials. *Annual Review of Materials Science*. 1999; 29:327-352. <http://dx.doi.org/10.1146/annurev.matsci.29.1.327>
21. Widegren J and Bergstrom L. The effect of acids and bases on the dispersion and stabilization of ceramic particles in ethanol. *Journal of the European Ceramic Society*. 2000; 20(6):659-665. [http://dx.doi.org/10.1016/S0955-2219\(99\)00199-5](http://dx.doi.org/10.1016/S0955-2219(99)00199-5)
22. Dorey RA and Whatmore RW. Electroceramic thick film fabrication for MEMS. *Journal of Electroceramics*. 2004; 12(1-2):19-32. <http://dx.doi.org/10.1023/B:JECR.00000033999.74149.a3>
23. Calderón-Colón X, Geng H, Gao B, An L, Cao G and Zhou O. A carbon nanotube field emission cathode with high current density and long-term stability. *Nanotechnology*. 2009; 20(325707):1-5.
24. Antonelli E, Letonturier M, M'Peko J-C and Hernandez AC. Microstructural, structural and dielectric properties of Er³⁺-modified BaTi_{0.85}Zr_{0.15}O₃ ceramics. *Journal of the European Ceramic Society*. 2009 29(8):1449-1455. <http://dx.doi.org/10.1016/j.jeurceramsoc.2008.09.009>